A Letters Journal Exploring the Frontiers of Physics

OFFPRINT

Anisotropic charge dynamics in detwinned $Ba(Fe_{1-x}Co_x)_2As_2$

A. Dusza, A. Lucarelli, F. Pfuner, J.-H. Chu, I. R. Fisher and L. Degiorgi

EPL, **93** (2011) 37002

A Letters Journal Exploring the Frontiers of Physics

February 2011

EPL, **93** (2011) 37002
doi: 10.1209/0295-5075/93/37002

www.epljournal.org

Anisotropic charge dynamics in detwinned $Ba(Fe_{1-x}Co_x)_2As_2$

A. Dusza[1(a)], A. Lucarelli[1(a)], F. Pfuner[1], J.-H. Chu[2,3], I. R. Fisher[2,3] and L. Degiorgi[1(b)]

[1] *Laboratorium für Festkörperphysik, ETH - Zürich, CH-8093 Zürich, Switzerland*
[2] *Geballe Laboratory for Advanced Materials and Department of Applied Physics, Stanford University Stanford, CA 94305-4045, USA*
[3] *Stanford Institute for Materials and Energy Sciences, SLAC National Accelerator Laboratory 2575 Sand Hill Road, Menlo Park, CA 94025, USA*

received on 6 January 2011; accepted by D. Vanmaekelbergh on 24 January 2011
published online 9 February 2011

PACS 74.70.Xa – Pnictides and chalcogenides
PACS 78.20.-e – Optical properties of bulk materials and thin films

Abstract – We investigate the optical conductivity with light polarized along the in-plane orthorhombic a and b axes of $Ba(Fe_{1-x}Co_x)_2As_2$ for $x = 0$ and 2.5% under uniaxial pressure across their structural and magnetic transitions. The charge dynamics at low frequencies and temperatures on these detwinned, single-domain samples reveals an enhancement of both the scattering rate and Drude weight of the charge carriers along the antiferromagnetic a-axis with respect to the ferromagnetic b-axis. Our findings also allow us to estimate the dichroism, which extends to high frequencies and temperatures. These results reveal a nematic susceptibility as well as the electronic nature of the structural transition.

A renewed interest in the study of symmetry-breaking competing states in complex interacting systems followed the discovery of a broken rotational symmetry, due to stripe or nematic order, in the pseudogap phase of the copper oxide superconductors [1]. The most recent playground in which to address the competition between structural, magnetic and superconducting phases is provided by the iron-pnictide superconductors [2,3]. In these systems, the non-superconducting parent compounds undergo an antiferromagnetic transition into a broken-symmetry ground state at T_N, which is always preceded by or coincident with a tetragonal-to-orthorhombic structural distortion at $T_s \geqslant T_N$ [4,5]. This latter transition implies a twofold electronic symmetry [6], which for a range of dopings coexists with superconductivity and long-range magnetic order [5]. Understanding the effects of the structural transition on the charge dynamics and the electronic bands by studying the optical properties of the system is an important step in order to develop a comprehensive theoretical description of these materials. However, the presence of dense structural domains which form below T_s hides the intrinsic electronic anisotropy of the orthorhombic phase that may be driven by a nematic order in the FeAs (a, b)-plane [6]. Indeed, naturally twinned samples present only an average of physical quantities, from which little detailed information can be extracted.

It has recently been demonstrated that single crystals of $Ba(Fe_{1-x}Co_x)_2As_2$ and also the parent compounds $BaFe_2As_2$ and $CaFe_2As_2$ [7,8] can be detwinned by application of uniaxial pressure, thus allowing investigations of the in-plane electronic anisotropy below T_s. Measurements of the resistivity of $Ba(Fe_{1-x}Co_x)_2As_2$ for currents flowing along the a and b axes (ρ_a and ρ_b, respectively) reveal a surprisingly large anisotropy, reaching a maximum value $\rho_b/\rho_a \sim 2$ for compositions close to the beginning of the superconducting dome (*i.e.* $x \sim 0.025$) [7]. At higher temperatures, the applied uniaxial pressure naturally breaks the 4-fold symmetry of the tetragonal state, such that the observed resistivity anisotropy extends above T_s, revealing the presence of a substantial "nematic susceptibility" [9–12]. Consequently, the sharp phase transition at T_s is changed into a broad crossover, due to the presence of the symmetry-breaking field [7].

In this letter we focus our attention on two specific compositions, $x = 0$ and $x = 0.025$. The former ($x = 0$) composition displays a small upturn in ρ_b at $T_s = T_N = 135\,\mathrm{K}$, while ρ_a suddenly decreases at this temperature. The latter ($x = 0.025$) composition is characterized by the onset of an insulating-like behavior of ρ_b somewhat above $T_s = 98\,\mathrm{K}$, for strained samples, while ρ_a decreases with decreasing temperature in a metallic-like fashion [7].

(a) Both authors equally contributed to the present work.
(b) E-mail: degiorgi@solid.phys.ethz.ch

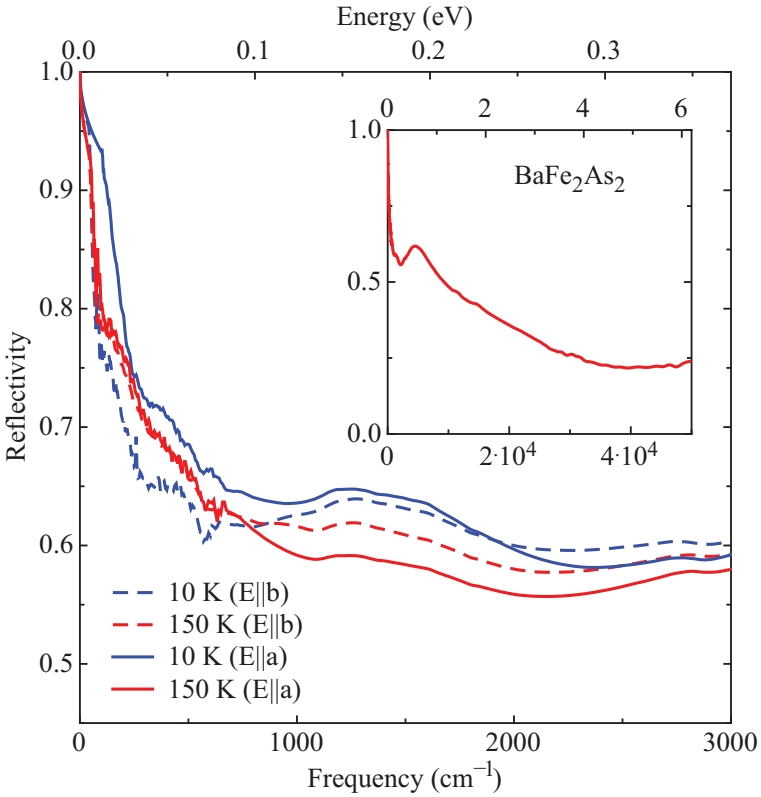

Fig. 1: (Color online) Optical reflectivity $R(\omega)$ for $x = 0$ at 10 and 150 K in the FIR and MIR range for both polarization directions. Inset: $R(\omega)$ up to the ultra-violet spectral range.

By means of the optical conductivity, obtained with light polarized along the a and b axes of samples under uniaxial pressure, we establish a substantial temperature-dependent anisotropy of the charge dynamics (*i.e.*, dichroism) which extends at $T > T_s$ and to frequencies up to the mid- and near-infrared (MIR and NIR, respectively) range, thus at energy scales well above $k_B T_s$. In addition, a significant and progressive depletion of spectral weight is observed between 200 and 700 cm^{-1} (previously ascribed to the opening of a spin-density-wave gap in studies of twinned samples [13]) for $E\|b$ but *not* for $E\|a$ on cooling below T_N. We furthermore discover that the metallic contribution to the excitation spectrum tracks the anisotropy observed in the temperature dependence of the dc transport properties along both axes. Specifically, the optical conductivity at far-infrared (FIR) frequencies at $T < T_s$ implies an enhanced Drude weight and scattering rate of the itinerant charge carriers along the a-axis with respect to the b-axis.

Similarly to ref. [7], we developed a detwinning device that allows optical measurements under constant uniaxial pressure. It consists of a mechanical clamp and an optical mask attached on top of it in tight contact. The pressure device was designed according to the following specific criteria [14]: i) it leaves the (001) facet of the single-domain samples exposed, enabling optical reflectivity ($R(\omega)$) measurements; ii) the optical mask guarantees data collection on surfaces of the same dimension for the sample and the reference mirror and therefore on equivalent flat spots; iii) the uniaxial stress is applied by tightening a screw and drawing the clamp against the side of the crystal, cut such that in the orthorhombic phase the a/b axes of the twinned samples would lie parallel to the stress direction; iv) the major axis of the tightening screw lies nearby and parallel to the surface of the sample so that the shear- and thermal-stress effects are minimized[1]. Cooling samples in this manner results in a significantly larger population of domains for which the shorter b-axis is oriented along the direction of the applied stress, almost fully detwinning the crystals. The applied pressure is modest such that T_N is unaffected, and can be adjusted over a limited range [7]. $R(\omega)$ data were thus collected as a function of temperature on these detwinned, single-domain samples in the spectral range between 30 and 6000 cm^{-1} [15]. Our data were complemented with room temperature measurements from NIR up to the visible and ultra-violet spectral range (3200–4.8×10^4 cm^{-1}). Light in all spectrometers was polarized along the a and b axes of the detwinned samples, thus giving access to

[1]The thermal expansion ΔL of the tightening screw, exerting the uniaxial pressure, can be estimated to be of the order of $\Delta L = \alpha L \Delta T = 20\,\mu$m (for screw length $L = 5$ mm, typical metallic thermal-expansion coefficient $\alpha = 2 \times 10^{-5}$ K^{-1}, and thermal excursion $\Delta T = 200$ K). This corresponds to a relative variation of about 0.4%. By reasonably assuming $\Delta L/L = \Delta p/p$, the influence of the thermal expansion is then negligible.

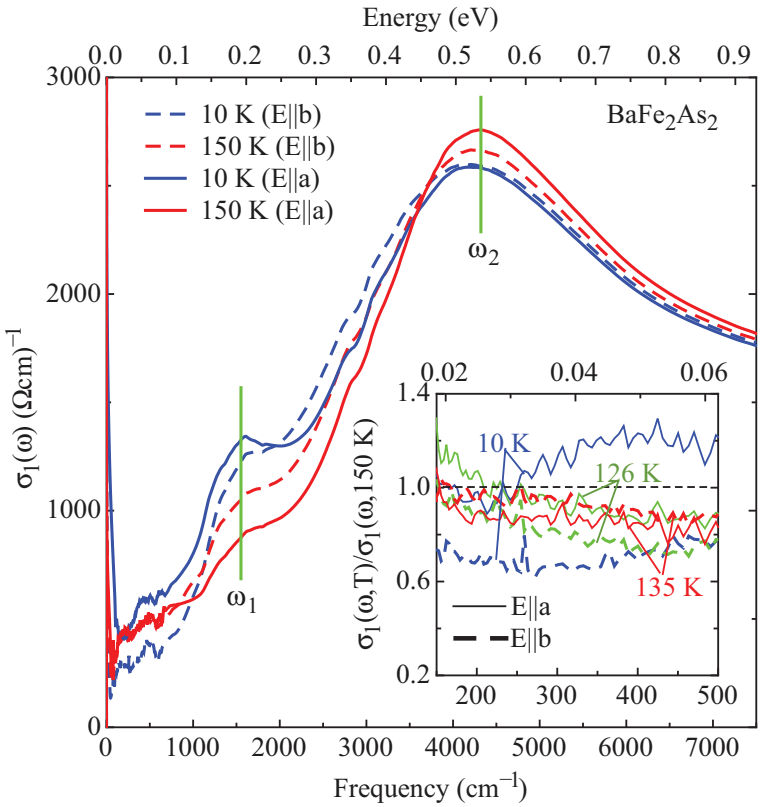

Fig. 2: (Color online) Real part $\sigma_1(\omega)$ of the optical conductivity at 10 and 150 K for $x = 0$ in the MIR-NIR range for both polarization directions. The vertical dashed lines mark the frequencies ω_1 and ω_2 (see text). Inset: ratio $\sigma_1(\omega, T < T_N)/\sigma_1(\omega, 150\,\mathrm{K})$ along the a and b axes.

the anisotropic optical functions. The real part $\sigma_1(\omega)$ of the optical conductivity was obtained via the Kramers-Kronig transformation of $R(\omega)$ by applying suitable extrapolations at low and high frequencies. For the $\omega \to 0$ extrapolation, we made use of the Hagen-Rubens (HR) formula ($R(\omega) = 1 - 2\sqrt{\frac{\omega}{\sigma_{\mathrm{dc}}}}$), inserting σ_{dc} values in fair agreement with ref. [7], while above the upper frequency limit $R(\omega) \sim \omega^{-s}$ ($2 \leqslant s \leqslant 4$) [15].

Prior to performing optical experiments as a function of the polarization of light, the electrodynamic response of the twinned (*i.e.*, unstressed) samples was first checked with unpolarized light, consistently recovering the same spectra previously presented in ref. [13]. Although the detwinning device does not permit a precise control of the applied pressure, the uniaxial stress was carefully increased enough to observe optical anisotropy, which was verified to disappear when the pressure was subsequently released[2]. The two compositions investigated displayed overall similar features in their optical response. To avoid repetition, raw data are shown only for $x = 0$. The discussion of the resulting dichroism is then performed for both compositions.

Figure 1 displays $R(\omega)$ of the $x = 0$ compound at $\omega < 3000\,\mathrm{cm}^{-1}$ for light polarized along the a and b axes at two selected temperatures, well above and below the phase transitions. The $R(\omega)$ spectra tend to merge together in the energy interval between 5000 and 6000 cm^{-1}. The inset illustrates the overdamped shape of the polarization-independent $R(\omega)$ in the visible and ultra-violet spectral range, already recognized in the twinned specimens [13]. The pronounced polarization dependence, leading to an optical anisotropy in the MIR-NIR range, persists up to temperatures of at least 200 K, thus well above all phase transitions. In the absence of evidence for any additional phase transitions at higher temperatures, this behavior presumably reflects a substantial nematic susceptibility for $T > T_s$. At FIR frequencies and approaching the zero-frequency limit, $R(\omega)$ is polarization independent above 150 K, while below 150 K it increases with decreasing temperature along the a-axis, consistent with the metallic character of the dc transport properties [7]. On the contrary, along the b-axis, there is a clear depletion of $R(\omega)$ at low temperatures in the energy range between 200 and 700 cm^{-1}, which is reminiscent of findings on the twinned samples [13]. $R(\omega)$ below 200 cm^{-1} displays a sharp upturn and consistently merges with the HR expectation from the

[2] As control measurement, we collect the optical reflectivity of a Cu sample of the same size (surface and thickness) of the pnictide crystals and in the same setup with the uni-axial pressure [14]. Figure 3(d) demonstrates, as expected, the total absence of dichroism in Cu.

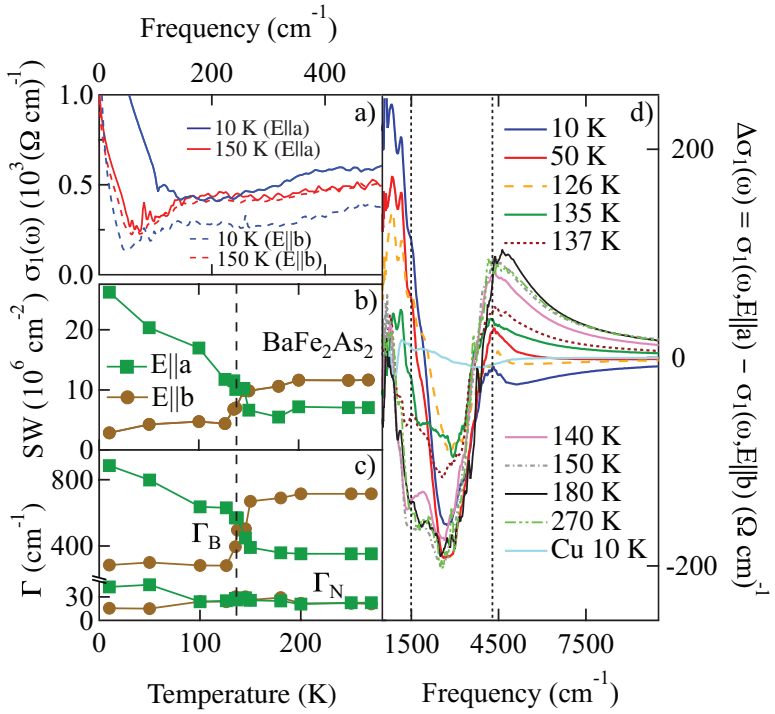

Fig. 3: (Color online) (a) Infrared part of $\sigma_1(\omega)$ at 10 and 150 K for both axes. Temperature dependence of the Drude spectral weight (SW) (b) and scattering rates Γ_N and Γ_B (c) along the a- and b-axis, extracted from the Drude-Lorentz fit of the optical response [13]. The vertical dashed line in both panels marks the phase transition at T_s. (d) Relative difference $\Delta\sigma_1(\omega)$ (dichroism) of the optical conductivity with polarization of light along the a- and b-axis at selected temperatures of the parent compound and of Cu at 10 K (see footnote [2]). The vertical dotted lines mark the frequencies ω_1 and ω_2 (fig. 2).

dc transport [7]. Another prominent feature in $R(\omega)$ is the strong polarization and temperature-dependent band at about 1500 cm^{-1}. An attentive look to the data (fig. 1) also reveals the interchange of the polarization dependence of $R(\omega)$ when crossing from high to low temperatures. Such an interchange occurs at $T = T_s$.

The real part $\sigma_1(\omega)$ of the optical conductivity of the parent compound at 10 and 150 K along both polarization directions is shown in fig. 2. Consistent with previous data [13], $\sigma_1(\omega)$ is dominated by the strong absorption peaked at about 4300 cm^{-1} and by the pronounced shoulder at 1500 cm^{-1} on its MIR frequency tail. An important result, evinced from our data, is the extension of the temperature-dependent optical anisotropy up to energies widely exceeding the energy scales set by the transition temperatures. The inset in fig. 2 shows $\sigma_1(\omega, T < T_N)/\sigma_1(\omega, 150\,\mathrm{K})$ for both a and b axes, which reinforces the opening of a pseudogap in the excitation spectrum for $E\|b$ at $T < T_N$, as anticipated by the depletion of $R(\omega)$ in FIR (fig. 1). This removes spectral weight, which principally piles up in the MIR feature at 1500 cm^{-1}. For $E\|a$, the spectral weight essentially moves from energies around the peak at 4300 cm^{-1} into the broad MIR shoulder at 1500 cm^{-1} and also down to low energies into the metallic contribution, so that $R(\omega)$ increases in the FIR range (fig. 1). This is explicitly emphasized in fig. 3(a), blowing up the FIR range of $\sigma_1(\omega)$ well above and below T_N. Our findings thus demonstrate that the magnetic transition at T_N seems to partially gap the portion of the Fermi surface pertinent to the b-axis response, while enhancing the metallic nature of the charge dynamics for the a-axis response.

A detailed analysis of the excitation spectrum was performed within the same Drude-Lorentz approach, previously introduced for the twinned samples [13] and adapted to both polarization directions. We limit here our attention to the metallic part of $\sigma_1(\omega)$ which consists of two (narrow (N) and broad (B)) Drude terms; the former is obviously tied to the zero-frequency extrapolation of $R(\omega)$, while the latter largely dominates the optical response [13]. The two Drude terms imply the existence of two electronic subsystems [16] and phenomenologically mimic the multi-band scenario in the iron-pnictides. Such an analysis reveals an enhancement (depletion) of the total Drude spectral weight along the $a(b)$-axis (fig. 3(b)). The corresponding scattering rates of the itinerant charge carriers increase along the antiferromagnetic a-axis, while they decrease along the ferromagnetic b-axis for $T < T_N$ (fig. 3(c)), as expected. Indeed, the large scattering rate along the a-axis may arise because of scattering by incoherent spin waves [17].

At this point, it is worth establishing the compelling comparison with the anisotropy ratio of the dc transport properties, defined as $\frac{\Delta\rho}{\rho} = \frac{2(\rho_b - \rho_a)}{(\rho_b + \rho_a)}$ [18]. From the Drude

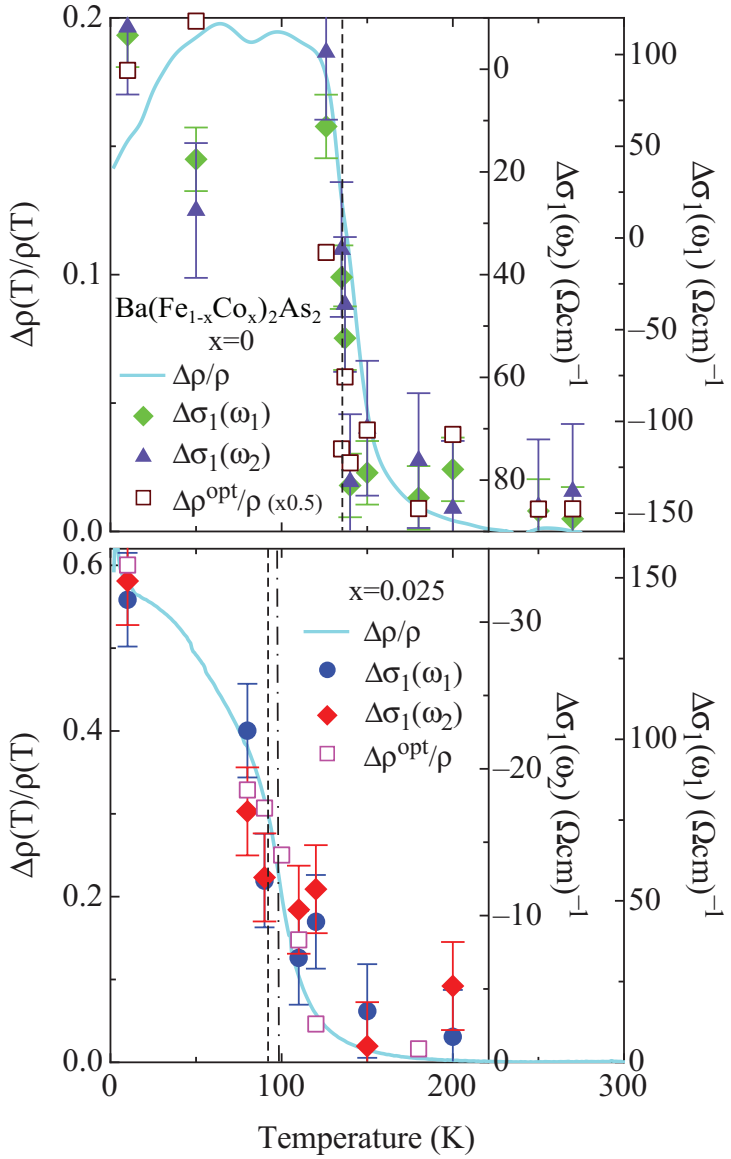

Fig. 4: (Color online) Temperature dependence of the dichroism $\Delta\sigma_1(\omega)$ for $x = 0$ and 0.025 at ω_1 and ω_2 (fig. 2) compared to $\frac{\Delta\rho}{\rho}$ from the dc transport data [7], as well as from the Drude terms in $\sigma_1(\omega)$ ($\frac{\Delta\rho^{opt}}{\rho}$). The vertical dashed and dash-dotted lines mark the magnetic and structural phase transitions at T_N and T_s, respectively.

terms we can estimate the dc limit of the conductivity ($\sigma_0^{opt} = (\omega_p^N)^2/4\pi\Gamma_N + (\omega_p^B)^2/4\pi\Gamma_B$, for both axes) more precisely than simply extrapolating $\sigma_1(\omega)$ to zero frequency. The anisotropy ratio $\frac{\Delta\rho^{opt}}{\rho}$, reconstructed from the optical data (*i.e.*, σ_0^{opt}), is thus compared in fig. 4 to the equivalent quantity from the transport investigation. The agreement in terms of $\frac{\Delta\rho}{\rho}$ between the optical and dc investigation is outstanding for $x = 0.025$ at all temperatures (fig. 4(b)), while $\frac{\Delta\rho^{opt}}{\rho}$ for $x = 0$ is larger at $T < T_s$ than from dc data (fig. 4(a)). This might originate from a stronger stress in the optical experiment than the one for the dc transport measurement [7]. Nonetheless, in order to account for the dc resistivity and its anisotropy along both axes, it appears that the anisotropy in the Fermi surface parameters (*i.e.*, Drude weights, fig. 3(b)) outweighs the anisotropy in the scattering rates (fig. 3(c)) that develops below T_N.

In order to emphasize the relevant polarization dependence at high frequencies, we calculate the difference $\Delta\sigma_1(\omega) = \sigma_1(\omega, E\|a) - \sigma_1(\omega, E\|b)$ at all measured temperatures. $\Delta\sigma_1(\omega)$, shown in fig. 3(d), represents an estimation of the dichroism and is very prominent in the MIR and NIR ranges (see footnote [2]). An anisotropy in the optical response for the magnetic state can be anticipated by *ab initio* calculations based on the density functional theory [19,20]. Because of the nematicity observed in the dc transport data at $T > T_s$ [7], it is interesting to compare the temperature dependence of the dc ($\frac{\Delta\rho}{\rho}$) and optical ($\Delta\sigma_1$) anisotropy. We select

the characteristic frequencies, identifying the position of the peaks in $\sigma_1(\omega)$; namely, $\omega_1 = 1500$ $(1320)\,\mathrm{cm}^{-1}$ and $\omega_2 = 4300$ $(5740)\,\mathrm{cm}^{-1}$ for $x = 0$ (0.025) (fig. 2). It is astonishing that the temperature dependence of $\Delta\sigma_1(\omega)$ at ω_1 and ω_2 follows remarkably well the temperature dependence of $\frac{\Delta\rho}{\rho}$ in both compounds (fig. 4). $\Delta\sigma_1(\omega_i)$ $(i = 1, 2)$ saturates at constant values well above T_s and then displays a sudden variation for $T < 2T_s$. Since the dichroism directly relates to a reshuffling of spectral weight in $\sigma_1(\omega)$ in the MIR-NIR range (fig. 2), $\Delta\sigma_1(\omega)$ at ω_1 is interrelated to that at ω_2; so that the behavior of $\Delta\sigma_1$ is monotonic as a function of temperature and opposite in sign between ω_1 and ω_2 (fig. 4). While $\Delta\sigma_1(\omega_i) = 0$ for $x = 0.025$ at $T > T_s$, $\Delta\sigma_1(\omega_i)$ for $x = 0$ is yet constant but different from zero, which may derive from an uniaxial pressure strong enough to induce an orbital polarization and thus a finite high-frequency dichroism already at $T \gg T_s$. Nonetheless, the impact of stronger pressure on $\Delta\sigma_1(\omega \to 0)$, at least for $x = 0$, seems to be negligible, or eventually beyond the precision of our FIR optical experiment, well above T_s but remarkable at $T < T_s$ (fig. 4(a)). However, contrary to the anisotropy in the dc resistivity, the absolute variation of the dichroism across the transitions at selected frequencies (figs. 3(d) and 4) is larger for $x = 0$ than for $x = 0.025$. This doping-dependence needs to be studied in a controlled pressure regime in order to exclude different degrees of detwinning. Even so, this result is certainly suggestive since the observed dichroism appears to have a similar doping dependence as the lattice orthorhombicity (*i.e.*, $(a-b)/(a+b)$) [21]. Our data might thus reveal a pronounced sensitivity of the electronic properties to structural parameters, like the iron-pnictogen angle [22].

The origin of the orthorhombic transition has been discussed from the closely related perspectives of spin fluctuations (a so-called spin nematic picture [9–12]), and also in terms of a more direct electronic effect involving, for instance, the orbital degree of freedom [18,23–26]. The present measurements alone cannot distinguish between these related scenarios, because in both cases some degree of electronic anisotropy is anticipated, and indeed it is likely that both effects play a combined role in the real material. Nevertheless, it is instructive to compare the observed dichroism with specific predictions made within a simple model based on orbital order. The two well-defined energy scales ω_1 and ω_2 (fig. 2) may represent optical transitions between states with the strongest d_{xz}/d_{yz} character, which are separated by about 0.3–0.4 eV. Such an energy splitting is indeed compatible with the theoretical calculations of the linear dichroism in the X-ray absorption spectroscopy [18].

In summary, the optical response of detwinned single crystals of the representative iron-arsenide $Ba(Fe_{1-x}Co_x)_2As_2$ displays an in-plane anisotropy which extends to relatively high frequencies and at $T > T_s$. This reveals a substantial nematic susceptibility as well as the electronic nature of the structural transition. A key result consists in the opportunity, offered by our optical investigation, to disentangle the distinct behaviors of the Drude weights and scattering rates along both axes, thus clarifying the striking $(\rho_b > \rho_a)$ dc anisotropy.

* * *

The authors wish to thank S. Kivelson, T. Devereaux, S. Massidda and D. Lu for fruitful discussions and J. Johannsen for valuable help in collecting part of the data. This work has been supported by the Swiss National Foundation for the Scientific Research within the NCCR MaNEP pool. This work is also supported by the Department of Energy, Office of Basic Energy Sciences under contract DE-AC02-76SF00515.

REFERENCES

[1] Daou R. *et al.*, *Nature*, **463** (2010) 519.
[2] Kamihara Y. *et al.*, *J. Am. Chem. Soc.*, **130** (2008) 3296.
[3] Rotter M. *et al.*, *Phys. Rev. Lett.*, **101** (2008) 107006.
[4] de la Cruz C. *et al.*, *Nature*, **453** (2008) 899.
[5] Lester C. *et al.*, *Phys. Rev. B*, **79** (2009) 144523.
[6] Tanatar M. A. *et al.*, *Phys. Rev. B*, **79** (2009) 180508.
[7] Chu J.-H. *et al.*, *Science*, **329** (2010) 824.
[8] Tanatar M. A. *et al.*, *Phys. Rev. B*, **81** (2010) 184508.
[9] Xu C. *et al.*, *Phys. Rev. B*, **78** (2008) 020501.
[10] Johannes M. and Mazin I., *Phys. Rev. B*, **79** (2009) 220510.
[11] Fernandes R. M. *et al.*, *Phys. Rev. Lett.*, **105** (2010) 157003.
[12] Fradkin E. *et al.*, *Annu. Rev. Condens. Matter Phys.*, **1** (2010) 153 and references therein.
[13] Lucarelli A. *et al.*, *New J. Phys.*, **12** (2010) 073036.
[14] http://www.spectro.ethz.ch/EPL/EPL37002.htm.
[15] Dressel M. and Grüner G., *Electrodynamics of Solids* (Cambridge University Press) 2002.
[16] Wu D. *et al.*, *Phys. Rev. B*, **81** (2010) 100512(R).
[17] Turner A. M. *et al.*, *Phys. Rev. B*, **80** (2009) 224504.
[18] Chen C.-C. *et al.*, *Phys. Rev. B*, **82** (2010) 100504(R).
[19] Yin Z. P. *et al.*, cond-mat/1007.2867.
[20] Sanna A. *et al.*, *Phys. Rev. B*, **83** (2011) 054502.
[21] Prozorov R. *et al.*, *Phys. Rev. B*, **80** (2009) 174517.
[22] Calderon M. T. *et al.*, *Phys. Rev. B*, **80** (2009) 09453.
[23] Krüger F. *et al.*, *Phys. Rev. B*, **79** (2009) 054504.
[24] Lee C.-C. *et al.*, *Phys. Rev. Lett.*, **103** (2009) 267001.
[25] Lv W. *et al.*, *Phys. Rev. B*, **82** (2010) 045125.
[26] Valenzuela B. *et al.*, *Phys. Rev. Lett.*, **105** (2010) 207202.